γ-soft rotor with configuration mixing in the O(6) limit of the interacting boson model

Feng Pan, Shuli Yuan, Zheng Qiao, Jiachao Bai, Yu Zhang, and Jerry P. Draayer

The γ-soft rotor with configuration mixing in the $O(6)$-limit of the interacting boson model

Feng Pan*,[1,2] Shuli Yuan,[1] Zheng Qiao,[1] Jiachao Bai,[1] Yu Zhang,[1] and Jerry P. Draayer[2]

[1]*Department of Physics, Liaoning Normal University, Dalian 116029, China*
[2]*Department of Physics and Astronomy, Louisiana State University, Baton Rouge, LA 70803-4001, USA*

Abstract: In order to describe obvious intruder states and nonzero quadrupole moments of γ-soft nuclei such as ^{194}Pt, a rotor extension plus intruder configuration mixing with $2n$-particle and $2n$-hole configurations from $n = 0$ up to $n \to \infty$ in the O(6) (γ-unstable) limit of the interacting boson model is proposed. It is shown that the configuration mixing scheme keeps lower part of the γ-unstable spectrum unchanged and generates the intruder states due to the mixing. It is further shown that almost all low-lying levels below 2.17MeV in ^{194}Pt can be well described by modifying the O(6) quadrupole-quadrupole interaction into an exponential form. The third order term needed for a rotor realization in the IBM seems necessary to produce nonzero quadrupole moments with the correct sign.

1. Introduction

It has been shown that the interacting boson model (IBM) is quite successful in the description of both collective valence shell [1] and multi-particle-hole [2–4] excitations in atomic nuclei. The IBM Hamiltonian can analytically be solved in the U(5) (vibrational), O(6) (γ-unstable), and SU(3) (rotational) limits. Each limit is associated with the corresponding level patterns and selection rules for transitions among excited states. Hence, the model is often adopted as benchmarks to simplify the analysis and interpretation of experimental data.

It has been shown [2, 3] that there are clear evidence for the presence of multi-particle-hole excitations in nuclei across the closed shells, in particular near closed-shell mass regions around proton number $Z \sim 50$ and $Z \sim 82$. Multi-particle-hole excitations are not easy to be incorporated in large-scale shell-model calculations due to the extremely large model space, which, however, can easily be handled within the IBM [5, 6]. IBM-2 in distinguishing neutron- from proton-pairs is often adopted in the configuration mixing schemes, of which calculations including up to 6-particle and 6-hole excitations have been carried out [7, 8]. The configuration mixing due to the multi-particle-hole excitations was considered in understanding shape coexistence phenomena by taking different symmetry limits of the IBM for different configurations [9–14]. These IBM-mixing calculations have been proven to be successful in describing intruder states and related phenomena in near closed shell nuclei, in which, however, many parameters are involved.

The purpose of this work is in two aspects. Firstly, it will be shown that a reasonably simplified configuration mixing scheme based on the O(6)-limit of the IBM-1 is analytically solvable, which could be useful in the analysis of experimental data of γ-soft nuclei such as ^{194}Pt. Secondly, it is demonstrated that the rotor extension [15, 16] in the O(6)-limit of the IBM seems necessary in order to produce nonzero quadrupole moments with correct sign and O(6)-limit forbidden E2 transitions. It is futher revealed that almost all low-lying levels below 2.17MeV in ^{194}Pt can be well described by modifying the O(6)-type quadrupole-quadrupole interaction with an exponential form.

2. A solvable configuration mixing scheme in the O(6)-limit

In the original IBM-1, which describes a system of fixed total number of s- and d-bosons subject to one- and two-body interactions, similar to the well-known consistent-Q (CQ) formalism, a typical Hamiltonian may be schematically written as [1]

$$\hat{H}_{\mathrm{CQ}} = \epsilon_d\,\hat{n}_d - \kappa\,\hat{Q}(\chi) \cdot \hat{Q}(\chi), \tag{1}$$

* The corresponding author's e-mail: daipan@dlut.edu.cn

where ϵ_d, κ, and $\chi \in [-\sqrt{7}/2, 0]$ are real parameters of the model, $\hat{n}_d = \sum_\mu d_\mu^\dagger d_\mu$ is the d-boson number operator, and $\hat{Q}_\mu(\chi) = d_\mu^\dagger s + s^\dagger \tilde{d}_\mu + \chi(d^\dagger \tilde{d})_\mu^{(2)}$ is the quadrupole operator, in which $(d^\dagger \tilde{d})_\mu^{(2)}$ stands for the $l = 2$ tensor coupling of the d-boson creation and annihilation operators with $\tilde{d} = (-)^\mu d_{-\mu}$, and $\hat{Q}(\chi) \cdot \hat{Q}(\chi) = \sum_\mu (-)^\mu \hat{Q}_\mu(\chi) \hat{Q}_{-\mu}(\chi)$.

There are three standard IBM-1 dynamical symmetry (limit) cases: the U(5)-limit for $\kappa = 0$, the SU(3)-limit for $\epsilon_d = 0$ and $\chi = -\sqrt{7}/2$, and the O(6)-limit for $\epsilon_d = 0$ and $\chi = 0$. In the O(6)-limit, for example, the eigenstates of (1) denoted as $|N, \sigma, \nu, \rho, L, M\rangle$ are nothing but the basis vectors of the group chain U(6)$\supset$O(6)$\supset$O(5)$\supset$O(3)$\supset$O(2), where N is the total number of bosons, σ is the O(6) quantum number, ν is the d-boson seniority number, ρ is an additional quantum number needed for the branching reduction of O(5)$\supset$O(3), and L and M are the quantum number of the angular momentum and that of its third projection, respectively.

Actually, besides the terms included in (1), other O(3) invariants, such as $\hat{L} \cdot \hat{L}$, where $\hat{L}_\mu$ are the angular momentum operators, can be considered. As will be shown later on, high order terms, such as $(\hat{L} \times \hat{Q} \times \hat{L})^{(0)}$ and $((\hat{L} \times \hat{Q})^{(1)} \times (\hat{L} \times \hat{Q})^{(1)})^{(0)}$, where $\hat{Q}_\mu \equiv \hat{Q}_\mu(0)$ are the generators of the O(6) group, may also be included. In such a case, the O(6)-symmetry is still preserved, but the O(5)-symmetry is broken. Eigenstates of such O(6)-limit Hamiltonian may be denoted as $|N, \sigma, \eta, L, M\rangle$, where η is an additional quantum number needed in the O(6) $\downarrow$ O(3) reduction.

The Hamiltonian suitable to describe $2n$-particle and $2n$-hole configuration mixing from $n = 0$ up to $n \to \infty$ in the extended O(6)-limit of the interacting boson model may be written as

$$\hat{H} = \hat{P}(2\Delta S^0 + \hat{H}_0 + g(S^+ + S^-))\hat{P}, \tag{2}$$

where $\hat{H}_0$ is an O(6)-limit Hamiltonian mentioned above, $S^0 = \frac{1}{2}(\hat{N} + 3)$, in which $\hat{N} = \hat{n}_d + \hat{n}_s$ is the total boson number operator with $\hat{n}_s = s^\dagger s$, $\Delta > 0$ represents the energy needed to excite two more particles from the closed shell resulting in a configuration with two more particles and two more holes, and is taken to be a constant for simplicity, $S^+ = S_d^+ - S_s^+$ ($S^- = (S^+)^\dagger$), in which $S_d^+ = \frac{1}{2}d^\dagger \cdot d^\dagger$ and $S_s^+ = \frac{1}{2}s^{\dagger 2}$ are the d- and s-boson pairing operator, respectively, and g is the mixing parameter, of which the allowed range will be shown later on, $\hat{P}$, satisfying $\hat{P}^2 = \hat{P}$ and $\hat{P}^\dagger = \hat{P}$, is the projection operator defined by

$$\hat{P}|N', \sigma, \eta, L, M\rangle = \begin{cases} |N', \sigma, \eta, L, M\rangle & \text{if } N' \geq N, \\ 0 & \text{otherwise}, \end{cases} \tag{3}$$

which keeps the Hamiltonian (2) to be effective only within the subspace spanned by $[N] \oplus [N+2] \oplus [N+4] \oplus \cdots$ mixed configurations, where N is the total boson number when no configuration mixing is considered, $|N', \sigma, \eta, L, M\rangle$ is the eigenstate of $\hat{H}_0$ with total number of bosons N'. (3) extends the projection introduced previously [5–14].

It should be noted that one can get two sets of SU(1,1) generators using the boson pairing operators $S_d^\pm$ and $S_s^\pm$. One is generated by S^+, S^-, and S^0, while another set is generated by $A^+ = S_d^+ + S_s^+$, $A^- = (A^+)^\dagger$, and S^0. These two sets of operators satisfy the same SU(1,1) commutation relations: $[S^0, S^\pm] = \pm S^\pm$, $[S^+, S^-] = -2S^0$, and $[S^0, A^\pm] = \pm A^\pm$, $[A^+, A^-] = -2S^0$. However, only $\{S^+, S^-, S^0\}$ are commutative with the O(6) generators [17]. The configuration mixing Hamiltonian used previously [5–14] was written as

$$\hat{H}_{\text{mix}} = g_s S_s^+ + g_d S_d^+ + g_s S_s^- + g_d S_d^-. \tag{4}$$

The coupling parameters g_s and g_d were all taken to be positive with $g_s > 0$ and $g_d > 0$, for example, shown in [5, 6], while the configuration mixing Hamiltonian adopted in (2) is equivalent to (4) with $g_s = -g_d = g > 0$. Since $S^\pm$ are commutative with the O(6) generators, and the $2n$-particle and $2n$-hole excitations are independent of the sign of g shown later on, the mixing term adopted in (2) greatly simplifies the calculation in the O(6)-limit of the IBM and keeps the nature of the $2n$-particle and $2n$-hole excitations unchanged.

The Casimir operator of the SU(1,1) generated by $\{S^+, S^-, S^0\}$ can be expressed as $C_2(SU(1,1)) = S^0(S^0 - 1) - S^+ S^-$. The basis vectors of $U(6) \supset O(6) \supset O(3)$ are simultaneously the basis vectors of the SU(1,1) generated by $\{S^+, S^-, S^0\}$. Under the basis vector $|N, \sigma, \eta, L, M\rangle$, the eigenvalue of $C_2(SU(1,1))$ and that of S_0 are given by

$$\begin{pmatrix} C_2(SU(1,1)) \\ S^0 \end{pmatrix} |N, \sigma, \eta, L, M\rangle = \begin{pmatrix} S(S-1) \\ \frac{1}{2}(N+3) \end{pmatrix} |N, \sigma, \eta, L, M\rangle \tag{5}$$

with $S = (\sigma + 3)/2$.

It can easily be verified that the Hamiltonian (2) can be solved exactly if eigenvalues of $\hat{H}_0$ are known. The first set of eigenstates labeled with an additional quantum number $\zeta = 1$, which are called normal states, is given by

$$|\zeta = 1, \omega\rangle = \mathcal{N}_{\zeta=1}\, e^{\alpha S^+} |N, \sigma, \eta, L, M\rangle, \tag{6}$$

where $\mathcal{N}_{\zeta=1}$ is the normalization factor, and $\omega \equiv \{N, \sigma, \eta, L, M\}$.

Since $[\hat{H}_0, S^+] = 0$, and $|N, \sigma, \eta, L, M\rangle$ is an eigenstate of $\hat{H}_0$, using the Hausdorff-Campbell relation

$$\hat{A}e^{\hat{B}} = e^{\hat{B}} \left(\hat{A} + \frac{1}{1!}[\hat{A}, \hat{B}] + \frac{1}{2!}[[\hat{A}, \hat{B}], \hat{B}] + \cdots \right), \tag{7}$$

we have

$$\hat{H}|\zeta = 1, \omega\rangle = \mathcal{N}_{\zeta=1}\, e^{\alpha S^+} \left(2\Delta\Lambda + \hat{H}_0 + 2\alpha\Delta S^+ + gS^+ + 2g\alpha\Lambda + g\alpha^2 S^+ \right) |N, \sigma, \eta, L, M\rangle, \tag{8}$$

where $\Lambda = \frac{1}{2}(N + 3)$. Hence, if $|\zeta = 1, \omega\rangle$ is an eigenstate of $\hat{H}$, the constant in the parentheses of (8) gives the corresponding eigen-energy with

$$E_{N,\sigma,\eta,L}^{(\zeta=1)} = \Delta(N + 3) + g\alpha(N + 3) + E_0(\sigma, \eta, L), \tag{9}$$

where $E_0(\sigma, \eta, L)$ is the eigenvalue of $\hat{H}_0$ under the eigenstate $|N, \sigma, \eta, L, M\rangle$, while the term proportional to S^+ in the parentheses of (8) must be zero, which leads to

$$g + 2\alpha\Delta + g\alpha^2 = 0 \tag{10}$$

with two possible solutions

$$\alpha^{\pm} = \frac{1}{g}(-\Delta \pm \sqrt{\Delta^2 - g^2}), \tag{11}$$

where $g \neq 0$ should be assumed. As shown in (10), when $g = 0$, $\alpha = 0$ is the only solution corresponding to the original O(6)-limit Hamiltonian without configuration mixing. Thus, the eigen-energy of (2) can be expressed as

$$E_{N,\sigma,\eta,L}^{(\zeta=1)} = (\pm)(N + 3)\sqrt{\Delta^2 - g^2} + E_0(\sigma, \eta, L) \tag{12}$$

corresponding to $\alpha = \alpha^{\pm}$. Since $\hat{H}$ is Hermitian, $\alpha^{\pm}$ must be real, which requires $|g| \leq \Delta$. It is obvious that the sign of g does not affect the eigen-energy (12).

Other sets of excited eigenstates (called intruder states) labeled with $\zeta \geq 2$, which is not possible in the O(6)-limit of the IBM without configuration mixing, also emerge due to the configuration mixing. For example, using the similar procedure, one can also get excited states of the first set of (2):

$$|\zeta = 2, \omega\rangle = \mathcal{N}_{\zeta=2}\, (1 + c\, S^+)e^{\alpha S^+}|\omega\rangle, \tag{13}$$

for fixed ω, where $\mathcal{N}_{\zeta=2}$ is the normalization factor, which implies $g \neq 0$. As shown in (2), when $g = 0$ there is no excited state similar to that shown in (13) built on the reference state $|\omega\rangle$. Namely, excited states with $\zeta > 1$ become null when $g = 0$. The corresponding eigen-energy of (2) under (13) is

$$E_{N,\sigma,\eta,L}^{(\zeta=2)} = E_{N,\sigma,\eta,L}^{(\zeta=1)} + 2g\, c\, \Lambda \tag{14}$$

with

$$c = \frac{2\Delta + 2g\alpha^{\pm}}{2g\Lambda} = \pm\frac{\sqrt{\Delta^2 - g^2}}{g\Lambda} \tag{15}$$

when $g \neq 0$. Substituting (15) into (14), we get

$$E_{N,\sigma,\eta,L}^{(\zeta=2)} = E_{N,\sigma,\eta,L}^{(\zeta=1)} \pm 2\sqrt{\Delta^2 - g^2} \tag{16}$$

for $g \neq 0$. Since physical spectrum should be lower-bound, only $\alpha = \alpha^+$ shown in (11) is possible, which corresponds to c given in (15) and the eigen-energy provided in (12) and (16) with positive sign. Otherwise, the spectrum will become upper-bound, which is non-physical and discarded. In (16), $2\sqrt{\Delta^2 - g^2}$ is the energy of the collective 2p-2h excitation. Again, the sign of g does not affect the 2p-2h excitation energy. In the following, $g > 0$ is always assumed.

It is obvious that there is an additional collective 2-particle and 2-hole excitation with energy $\mathbf{\Delta}_{2p2h} = 2\sqrt{\Delta^2 - g^2}$, which is absent in the original O(6)-limit description. Since the energy needed to excite two more particles from the closed shell resulting in the configuration with two more particles and two more holes is relatively large, the excited levels with $\zeta \geq 3$ lie much higher in energy, which are not considered in the following. It is clear that the spectrum generated from (2) with the configuration mixing keeps the lower part of the spectrum to be the same as that generated from the O(6)-limit of the IBM, while there are a set of the O(6)-type levels with the band heads provided by the $2n$-particle and $2n$-hole excitations, of which some low-lying levels are shown in Fig. 1. It is clearly shown that the first set of levels with $\zeta = 1$ are the same as those generated from the model without configuration mixing ($g = 0$), the second set of levels with $\zeta = 2$ are built on the 0_4^+ level with the gap $\mathbf{\Delta}_{2p2h}$ to the ground level, and so on. Each set of the levels with $\zeta \geq 2$ is a replica of those with $\zeta = 1$ generated from the original O(6)-limit without configuration mixing, but there are energy gaps among different sets.
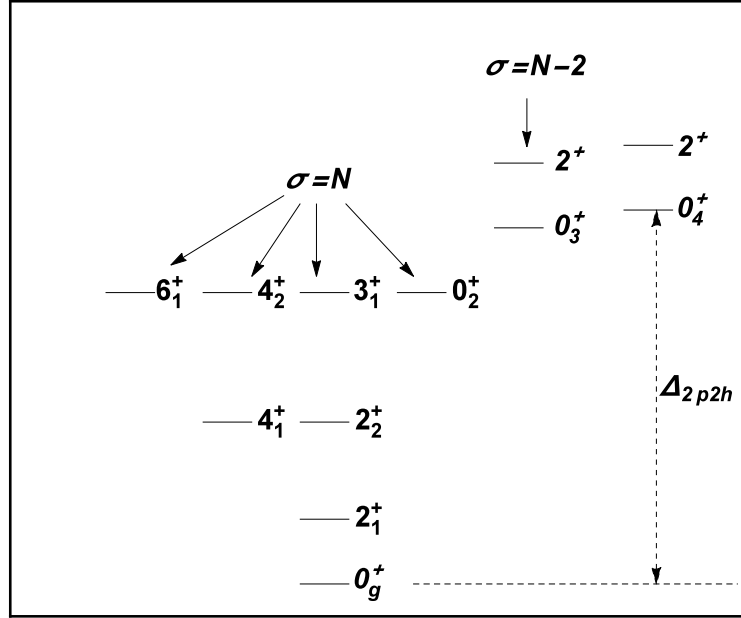

FIG. 1: (Color online) Low-lying level pattern of the solvable configuration mixing O(6) model with the Hamiltonian given by (2), where the left 10 levels are the same as those generated from the O(6)-limit of the IBM with the first term of (2) only, which, up to a constant, is typically given by $\hat{H}_0 = -\kappa \hat{Q} \cdot \hat{Q}$ with eigen-energy $E_0 = -\kappa(\sigma(\sigma + 4) - \nu(\nu + 3))$, where κ is a scale parameter, and ν is the seniority number of the O(5) group. Only levels of normal states with ($\sigma = N, \nu \leq 3$), ($\sigma = N - 2, \nu \leq 1$), and intruder levels with $\nu \leq 1$ are shown. 0_4^+ is the intruder state of the model with $\mathbf{\Delta}_{2p2h} = 2\sqrt{\Delta^2 - g^2}$.

It is clear that the eigenstates (6), (13), *etc* are the SU(1,1) coherent states built on the O(6)-limit eigenstate of the IBM due to the projection (3). As a consequence, matrix elements of any operator in the model can be derived analytically. For example, one can prove that the norm

$$\langle \omega | e^{\alpha \tilde{S}^-} e^{\beta \tilde{S}^+} | \omega \rangle = (1 - \alpha\beta)^{-N-3}, \tag{17}$$

which only depends on N. Hence, we have

$$\mathcal{N}_{\zeta=1} = (1-\alpha^2)^{(N+3)/2}. \tag{18}$$

One can also derive

$$\langle \zeta=1, \omega|S^\pm|\zeta=1, \omega\rangle = (\mathcal{N}_{\zeta=1})^2 \, \tfrac{\partial}{\partial\alpha}\langle\omega|e^{\alpha\tilde{S}^-}e^{\beta\tilde{S}^+}|\omega\rangle\Big|_{\beta=\alpha} = (\mathcal{N}_{\zeta=1})^2 \, \tfrac{\partial}{\partial\beta}\langle\omega|e^{\alpha\tilde{S}^-}e^{\beta\tilde{S}^+}|\omega\rangle\Big|_{\beta=\alpha}. \tag{19}$$

Thus, one can prove that

$$\langle \zeta', \omega'|\zeta, \omega\rangle = \delta_{\zeta', \zeta}\,\delta_{\omega', \omega}. \tag{20}$$

Similarly, the normalization factor of (13) can be expressed as

$$\mathcal{N}_{\zeta=2} = \sqrt{\frac{(\alpha^2-1)\alpha}{c}}\,\mathcal{N}_{\zeta=1} = \sqrt{\alpha^2(N+3)}\,\mathcal{N}_{\zeta=1}. \tag{21}$$

Due to the configuration mixing, the operator of the total number of bosons $\hat{N}$ is not a conserved quantity. The degree of the configuration mixing may be measured by the expectation value and fluctuation of $\hat{N}$ for a given state defined as

$$\bar{N} = \tfrac{1}{N}\langle \zeta, N, \sigma, \eta, L, M|\hat{N}|\zeta, N, \sigma, \eta, L, M\rangle,$$

$$\delta N = \tfrac{1}{N}\left(\langle \zeta, N, \sigma, \eta, L, M|\hat{N}^2|\zeta, N, \sigma, \eta, L, M\rangle - \bar{N}^2\right)^{\frac{1}{2}}. \tag{22}$$

For the ground state with $\sigma = N$, $\eta = 1$, and $L = 0$, (22) can be expressed explicitly as

$$\bar{N}_{\zeta=1} = 1 - \tfrac{2\alpha}{cN}, \tag{23}$$

$$\delta N_{\zeta=1} = \tfrac{2}{N}\sqrt{\tfrac{\alpha}{c(\alpha^2-1)}} = \tfrac{2}{cN}\sqrt{\tfrac{1}{N+3}}. \tag{24}$$

It can be expected that the mixing is mainly driven by the mixing term in the Hamiltonian (2) with the mixing parameter g. When $g = 0$, $\bar{N}_{\zeta=1} = 1$ and $\delta N_{\zeta=1} = 0$ indicating that the system is in the O(6)-limit without configuration mixing. With the increasing of $g > 0$, the mixing occurs with $\bar{N}_{\zeta=1} > 1$ and $\delta N_{\zeta=1} > 0$. Though both $\bar{N}$ and δN increase with the increasing of g with $0 < g < \Delta$, the increasing in $\bar{N}$ with the increasing of g is more noticeable. The expectation value of the total number of bosons of the first excited intruder state with $\sigma = N$, $\eta = 2$, and $L = 0$ corresponding to 0_4^+ state shown in the caption of Fig. 1 can also be derived, which is given by

$$\bar{N}_{\zeta=2} = \tfrac{1}{N}\langle \zeta=2|\hat{N}|\zeta=2\rangle =$$
$$\tfrac{N+2}{N} + \tfrac{2\alpha^2(\alpha^2-1)}{Nc}\left(\tfrac{1}{\alpha(\alpha^2-1)} + \tfrac{1}{c} + \tfrac{\alpha}{\alpha^2-1} - (\alpha + \tfrac{2c}{\alpha^2-1})(\tfrac{1}{\alpha c} + \tfrac{1}{\alpha^2-1})\right). \tag{25}$$

In this case, $g \neq 0$ should be assumed. When $g \to 0$, $\bar{N}_{\zeta=2} \to 1 + 2/N$ indicating that the collective 2p-2h excitation component dominates in the 0_4^+ state. With the increasing of $g > 0$, the mixing of $[N+2m]$ configurations with $m \geq 2$ in this intruder state occurs with $\bar{N}_{\zeta=2} > 1 + 2/N$. Since the increasing in $\bar{N}_\zeta$ with the increasing of g is more noticeable, only $\bar{N}_\zeta$ with $\zeta = 1$ and $\zeta = 2$ are shown in Fig. 2. As shown in Fig. 2, the ground state with $\zeta = 1$ is dominated by the $[N]$ configuration, while 0_4^+ state with $\zeta = 2$ is dominated by the $[N+2]$ configuration, as long as the mixing parameter is small with $g \sim 0$.

It can be understood that the differences of the mixing scheme with infinite number of configurations considered in this work from those with finite number of configurations studied previously are in two aspects. Firstly, the eigen-energies and eigen-states of the two schemes are quite the same, but the number of excitations $\zeta_{\max}$ should be terminated in the latter. For example, when $m+1$ configurations $[N] \oplus [N+2] \oplus [N+4] \oplus \cdots \oplus [N+2m]$ are adopted, the projection $\hat{P}$ should be restricted by another additional condition with $\hat{P}|N', \omega\rangle = 0$ for $N' > N + 2m$. Hence, the term $\exp[\alpha S^+]$ in (6) and (13) in this case is equivalent to its Taylor expansion in terms of α with $m+1$ terms due to the projection, resulting in a system with finite number of collective 2-particle and 2-hole excitations.
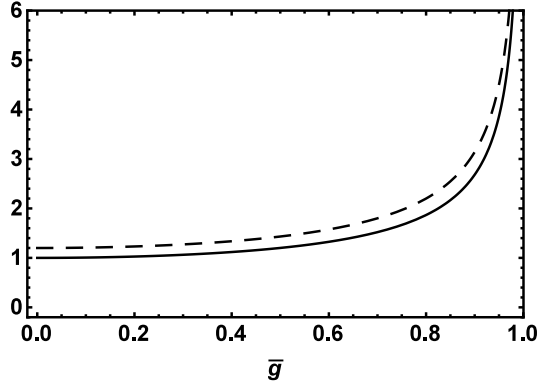
FIG. 2: (Color online) The ground state expectation value of the total number of bosons $\bar{N}_{\zeta=1}$ given by (23) (solid curve) and the expectation value of the total number of bosons of the first intruder 0_4^+ state $\bar{N}_{\zeta=2}$ given by (25) (dashed curve) as functions of the mixing parameter $\bar{g} = g/\Delta_0$, where Δ_0 is an arbitrary scale factor, and $\bar{\Delta} = \Delta/\Delta_0$. $N = 10$ and $\bar{\Delta} = 1$ are taken in the plot.

Secondly, the Taylor expansion in terms of α for the norm $\mathcal{N}$ with $m+1$ terms in the current scheme is equivalent to that in the mixing scheme with finite number of configurations if the same form of the eigenstates is adopted, though there will be a little difference in the result due to the finite term cutoff. Since physical quantities, such as B(E2) values, are related to the norms involved, the results of the Taylor expansion for the norms involved with $m+1$ terms are similar to those of the mixing scheme with $m + 1$ configurations. Since $g/\Delta < 1$ is always satisfied, there is no much difference of the exact results provided in this work from those with the finite-term Taylor expansions because $\alpha \sim -g/(2\Delta)$ is a small quantity, which justifies that the configuration mixing scheme with infinite number of configurations is acceptable.

As shown in [5–14], the effective boson charge needs to be taken with different values for different multi-particle-hole configurations. The E2 operator used in this work is simply chosen as

$$T_\mu(\mathrm{E2}) = q_2 \hat{P}_N \hat{Q}_\mu \hat{P}_N + q_2' \hat{P} \hat{Q}_\mu \hat{P}, \tag{26}$$

where $\hat{P}_N$ is a projection onto the configuration without multi-particle-hole excitations, with which the B(E2) values are given by

$$\mathrm{B}(\mathrm{E2}; \omega_i, L_i \to \omega_f, L_f) = \frac{1}{2L_i + 1} |\langle \omega_f, L_f \| T(\mathrm{E2}) \| \omega_i, L_i \rangle|^2, \tag{27}$$

where ω_i and ω_f stand for other relevant quantum numbers involved.

Similar to the O(6)-limit of the model without configuration mixing, reduced matrix elements of any operator in the model can be derived analytically when the O(5)-symmetry is preserved. In this case, the reduced matrix elements of $T(\mathrm{E2})$ operators for the transition between the normalized normal or intruder states under the $U(6) \supset O(6) \supset O(5) \supset O(3)$ basis can be expressed as

$$\langle \zeta = 1, N', \sigma', \nu', \rho', L' \| T(\mathrm{E2}) \| \zeta = 1, N, \sigma, \nu, \rho, L \rangle$$
$$= \delta_{NN'} \delta_{\sigma\sigma'} q_2((\mathcal{N}_{\zeta=1})^2 + \lambda) \langle N, \sigma', \nu', \rho', L' \| \hat{Q} \| N, \sigma, \nu, \rho, L \rangle, \tag{28}$$

$$\langle \zeta = 2, N', \sigma', \nu', \rho', L' \| T(\mathrm{E2}) \| \zeta = 2, N, \sigma, \nu, \rho, L \rangle$$
$$= \delta_{NN'} \delta_{\sigma\sigma'} q_2(\alpha^2(N+3)(\mathcal{N}_{\zeta=1})^2 + \lambda) \langle N, \sigma', \nu', \rho', L' \| \hat{Q} \| N, \sigma, \nu, \rho, L \rangle, \tag{29}$$

while those for the transitions between the normalized normal and intruder states are given by

$$\langle \zeta = 1, N', \sigma', \nu', \rho', L' \| T(\mathrm{E2}) \| \zeta = 2, N, \sigma, \nu, \rho, L \rangle$$
$$= \delta_{NN'} \delta_{\sigma\sigma'} q_2 \sqrt{\alpha^2(N+3)} (\mathcal{N}_{\zeta=1})^2 \langle N, \sigma', \nu', \rho', L' \| \hat{Q} \| N, \sigma, \nu, \rho, L \rangle, \tag{30}$$

where $\lambda = q_2'/q_2$.

When high order terms $(\hat{L} \times \hat{Q} \times \hat{L})^{(0)}$ and $((\hat{L} \times \hat{Q})^{(1)} \times (\hat{L} \times \hat{Q})^{(1)})^{(0)}$ are included in $\hat{H}_0$ as shown in the next section, the eigenstates of $\hat{H}_0$ may be expressed as

$$|N, \sigma, \eta, L, M\rangle = \sum_{\nu, \rho} C^{(\eta)}_{\nu, \rho} |N, \sigma, \nu, \rho, L, M\rangle \tag{31}$$

where $|N, \sigma, \nu, \rho, L, M\rangle$ is the basis vectors of $U(6) \supset O(6) \supset O(5) \supset O(3)$, and $C^{(\eta)}_{\nu, \rho}$ is the corresponding expansion coefficient, which can be obtained by diagonalizing the Hamiltonian $\hat{H}_0$ in the $U(6) \supset O(6) \supset O(5) \supset O(3)$ basis. The additional quantum number η labels the η-th eigenstate of $\hat{H}_0$ for fixed σ and L. For this case, the reduced matrix elements of $T(E2)$ needed in the next section may be expressed as

$$(\zeta = 1, N', \sigma', \eta', L' \| T(E2) \| \zeta = 1, N, \sigma, \eta, L)$$
$$= \delta_{NN'} \delta_{\sigma\sigma'} \, q_2 ((\mathcal{N}_{\zeta=1})^2 + \lambda) \sum_{\nu', \rho', \nu, \rho} C^{(\eta')}_{\nu', \rho'} C^{(\eta)}_{\nu, \rho} \langle N, \sigma', \nu', \rho', L' \| \hat{Q} \| N, \sigma, \nu, \rho, L \rangle \tag{32}$$

and

$$(\zeta = 1, N', \sigma', \eta', L' \| T(E2) \| \zeta = 2, N, \sigma, \eta, L)$$
$$= \delta_{NN'} \delta_{\sigma\sigma'} \, q_2 \sqrt{\alpha^2(N+3)} (\mathcal{N}_{\zeta=1})^2 \sum_{\nu', \rho', \nu, \rho} C^{(\eta')}_{\nu', \rho'} C^{(\eta)}_{\nu, \rho} \langle N, \sigma', \nu', \rho', L' \| \hat{Q} \| N, \sigma, \nu, \rho, L \rangle. \tag{33}$$

The reduced matrix element $\langle N, \sigma', \nu', \rho', L' \| \hat{Q} \| N, \sigma, \nu, \rho, L \rangle$ involved in (28)-(30) and (32)-(33) can further be expressed as [18]

$$\langle N, \sigma, \nu', \rho', L' \| \hat{Q} \| N, \sigma, \nu, \rho, L \rangle = \sqrt{2L'+1} \langle N, \sigma, \nu' \| \hat{Q} \| N, \sigma, \nu \rangle \langle \nu, \rho, L; 1, 2 \| \nu', \rho', L' \rangle \tag{34}$$

with

$$\langle N, \sigma, \nu' \| \hat{Q} \| N, \sigma, \nu \rangle = \begin{cases} (\sigma(\sigma+4) - \nu(\nu+4))^{1/2} \sqrt{\frac{\nu+1}{2\nu+5}}, & \text{for } \nu' = \nu+1, \\[2mm] (\sigma(\sigma+4) - (\nu-1)(\nu+3))^{1/2} \sqrt{\frac{\nu+2}{2\nu+1}}, & \text{for } \nu' = \nu-1, \end{cases} \tag{35}$$

where $\langle \nu, \rho, L; 1, 2 \| \nu', \rho', L' \rangle$ is the elementary Wigner coefficient (isoscalar factor) of $O(5) \supset O(3)$, which was given, for example, in [19, 20]. The reduced matrix elements and the elementary Wigner coefficients of $O(5) \supset O(3)$ satisfy the following relations:

$$\langle N, \sigma, \nu' \| \hat{Q} \| N, \sigma, \nu \rangle = \sqrt{\frac{\dim[\nu]}{\dim[\nu']}} \langle N, \sigma, \nu \| \hat{Q} \| N, \sigma, \nu' \rangle, \tag{36}$$

$$\langle N, \sigma, \nu', \rho', L' \| \hat{Q} \| N, \sigma, \nu, \rho, L \rangle = (-1)^{L+2-L'} \langle N, \sigma, \nu, \rho, L \| \hat{Q} \| N, \sigma, \nu', \rho', L' \rangle, \tag{37}$$

and

$$\langle \nu, \rho, L; 1, 2 \| \nu', \rho', L' \rangle = (-1)^{L'+2-L} \sqrt{\frac{\dim[\nu'](2L+1)}{\dim[\nu](2L'+1)}} \langle \nu', \rho', L'; 1, 2 \| \nu, \rho, L \rangle, \tag{38}$$

where

$$\dim[\nu] = \frac{1}{6}(\nu+1)(\nu+2)(2\nu+3) \tag{39}$$

is the dimension of the $O(5)$ irreducible representation $(\nu, 0)$. In the $O(5)$-symmetry preserved case shown above, since N is a finite number and α is small, the transitions among both normal and intruder states are similar to those in the

O(6)-limit without configuration mixing. The E2 selection rules are quite the same as those given in the O(6)-limit without configuration mixing, which are given by $\delta\sigma = 0$, and $\delta\nu = 0$ or ± 1.

3. Application to ^{194}Pt

In the IBM description, the Platinum isotopes are mainly within the $U(5)$-$O(6)$ transitional region. As shown in previous works [21, 22], the U(5) ingredient in even-even $^{172-194}$Pt is not negligible, especially in the isotopes with the mass number $A \leq 190$. Therefore, though the presence of intruder states in even-even $^{182-184}$Pt is much more evident, the current model based on the O(6)-limit is only suitable to describe ^{194}Pt which is nearest to the O(6)-limit point of the Casten triangle [21, 22]. Among the Platinum isotopes, there are abundant data of reduced E2 transition matrix elements, quadrupole moments, and B(E2) values of ^{194}Pt obtained from Coulomb excitations [23, 24], which are very much helpful for a detailed analysis. Hence, ^{194}Pt is chosen as an example to be described by the O(6)-limit Hamiltonian (2). The Platinum isotopes were studied earlier in the IBM-2 framework [25], in which only excited sates in the ground band up to 8_1^+, a few excited states in the quasi-β and quasi-γ bands were considered, and only quadrupole moment of 2_1^+ state was calculated. The shape evolution in Platinum isotopes was investigated [21] by using the extended consistent-Q formalism (ECQF) of the IBM, in which intruder configuration was not taken into account. Level patterns and B(E2) ratios of the isotopes were globally fitted rather well in [21]. However, the possible intruder state 0_4^+ and so on in ^{194}Pt were excluded. A comparison of the results of the IBM plus configuration mixing (IBM-CM) with those of the ECQF was made in [22], in which the 0_4^+ in ^{194}Pt was considered. In both [21] and [22], only excited states with excitation energy below 1.5MeV in ^{194}Pt were included. It can be observed that the level energy of 5_1^+ state in both the IBM-CM and the ECQF shown in [22] is 0.5-0.7MeV higher than the corresponding experimental value. Actually, there are 4^+, 5^+, 6^+, and 8^+ states with excitation energy $\sim$ 2.0MeV. It can be expected that level energies of other excited states with higher angular momentum quantum numbers provided from both the IBM-CM and the ECQF calculations would also be much higher than the corresponding experimental values. Moreover, similar to the original O(6)-limit case in the IBM-1, quadrupole moments of low-lying states calculated from the IBM-CM are zero, while those calculated from the ECQF are all with opposite sign.

Based on the above observations, we propose the following $O(6)$-limit Hamiltonian for the purpose:

$$\hat{H}_0 = -\kappa_0\, e^{\xi\,\hat{Q}\cdot\hat{Q}}\hat{Q}\cdot\hat{Q} + a\,\hat{L}^2 + b\,X_3 + d\,X_4, \tag{40}$$

where $\kappa_0 > 0$, $0 < \xi \ll 1$, $a > 0$, b, and d are free parameters,

$$X_3 = \frac{\sqrt{30}}{6}\,(\hat{L} \times \hat{Q} \times \hat{L})^{(0)}, \tag{41}$$

and

$$X_4 = -\frac{5\sqrt{3}}{18}\,((\hat{L} \times \hat{Q})^{(1)} \times (\hat{L} \times \hat{Q})^{(1)})^{(0)}. \tag{42}$$

The quadrupole-quadrupole interaction in the original O(6)-limit of the IBM-1 is replaced by the exponential form shown in (40), which is effective to produce relatively lower excitation energies of excited states with large d-boson seniority numbers. A similar exponential form of $\hat{Q} \cdot \hat{Q}$ was introduced in [26] for the symplectic no-core shell-model calculations, which justifies the IBM form used in (40) is reasonable as long as the parameter $\xi \ll 1$. The third and fourth order terms X_3 and X_4 in (40) are originated from the mapping result of a triaxial rotor Hamiltonian to that of the SU(3)-limit in the IBM [15, 16]. Though the quadrupole operator in the SU(3)-limit and that in the O(6)-limit are different, they are quite the same in the large-N limit. Therefore, the second to the fourth terms of (40) are also equivalent to a rotor image in the IBM. Since the quadrupole operators used in (40) are the generators of O(6), the model described by (40) is called the γ-soft rotor. It is obvious that the third and the fourth order terms keep the O(6)-symmetry, but break the O(5)-symmetry. As a result, the selection rules for the reduced matrix elements of $\hat{Q}$ between eigenstates of (40) are altered. Especially, besides nonzero reduced matrix elements with $\delta\sigma = 0$ and $\delta\nu = \pm 1$, the reduced matrix elements with $\delta\sigma = 0$ and $\delta\nu = 0$ or ± 2 could also be nonzero. For this case, the eigenstate of (40) is given by (31).

It is shown [27] that the coherent state method is able to establish a correspondence between quantum variables and classical (geometrical) variables, with which the classical equilibrium shapes and their evolution of a nucleus

described by the IBM have been studied [28, 29]. In order to show the potential shape of (40) in the classical limit, we use the standard coherent state defined as [30]

$$|N, \beta, \gamma\rangle = (N!(1+\beta^2)^N)^{-\frac{1}{2}} \left(s^\dagger + \beta \cos\gamma \, d_0^\dagger + \frac{1}{\sqrt{2}}\beta \sin\gamma \, (d_2^\dagger + d_{-2}^\dagger)\right)^N |0\rangle \qquad (43)$$

to obtain the scaled potential surface of the four terms involved in (40) in the large-N limit. Since $\xi \ll 1$, the first term of (40) can be expressed as

$$-\kappa_0 \, e^{\xi \, \hat{Q}\cdot\hat{Q}} \hat{Q}\cdot\hat{Q} = -\kappa_0 \left(\hat{Q}\cdot\hat{Q} + \xi(\hat{Q}\cdot\hat{Q})^2 + \frac{1}{2}\xi^2(\hat{Q}\cdot\hat{Q})^3 + \cdots\right) \qquad (44)$$

after the Taylor expansion around $\xi = 0$. Though the expectation value of (44) under (43) can not be evaluated easily, the expectation value of each term in the expansion shown in (44) is given by

$$\frac{1}{N^2}\langle Q\cdot Q\rangle\big|_{N\to\infty} = \frac{4\beta^2}{(1+\beta^2)^2}, \quad \frac{1}{N^4}\langle(Q\cdot Q)^2\rangle\big|_{N\to\infty} = \frac{16\beta^4}{(1+\beta^2)^4}, \quad \cdots, \quad \frac{1}{N^{2k}}\langle(Q\cdot Q)^k\rangle\big|_{N\to\infty} \sim \frac{\beta^{2k}}{(1+\beta^2)^{2k}}. \qquad (45)$$

Namely, the classical potential of the first term of (40), similar to that of the $\hat{Q}\cdot\hat{Q}$ in the O(6)-limit, is γ-independent. The expectation values of the second and the fourth terms are given by

$$\frac{1}{N}\langle\hat{L}^2\rangle\big|_{N\to\infty} = \frac{6\beta^2}{1+\beta^2}, \quad \frac{1}{N^3}\langle X_4\rangle\big|_{N\to\infty} = \frac{2\beta^4}{3(1+\beta^2)^3}, \qquad (46)$$

which are also γ-independent. While The expectation value of the third term is

$$\frac{1}{N^2}\langle X_3\rangle\bigg|_{N\to\infty} = -\frac{2\beta^3}{(1+\beta^2)^2}\cos(3\gamma). \qquad (47)$$

In contrast to the SU(3)-limit case shown in [15, 16], there is no triaxial shape emerging from (40). Since the X_3 term in the classical limit is proportional to $\cos(3\gamma)$, similar to the SU(3)-limit of the IBM-1, only axial deformation with $\gamma = 0$ or $\gamma = \pi/3$ is possible. Hence, if the parameters of the Hamiltonian (40) are appropriately scaled with N, the shape at the ground state of this model is axially deformed with either prolate ($\gamma = 0$) when $b > 0$ or oblate ($\gamma = \pi/3$) when $b < 0$ in the large-N limit as estimated by the coherent state description.

Using the γ-soft rotor Hamiltonian (40), we are able to describe level energies of ^{194}Pt up to 2.17MeV. We observe that the parameter d taken to be 0 is always better as far as the level energies are concerned, so that the X_4 term in (40) can be removed for ^{194}Pt. The other parameters used are $\kappa_0 = 7.3$ keV, $\xi = 0.0178$, $a = 10$ keV, and $b = -4.5$ keV, while the gap $\mathbf{\Delta}_{2p2h} = 2\sqrt{\Delta^2 - g^2} = 1.547$MeV is fixed according to the 0_4^+ level energy, from which the parameter $\Delta > 0$ can be expressed as $\Delta = \sqrt{0.5983 + g^2}$, where Δ and g are in MeV. The mixing parameter g is then fixed from a global fits to the reduced T(E2) matrix elements (32) and (33) which depend on Δ and g according to (11). The fitting results of the level energies up to 2.17MeV in comparison to the corresponding experimental data are shown in Table I. It can be checked against the experimental level energies shown in [24] that most level energies of positive parity states are fitted rather well. With excitation energy below 2.17MeV, negative parity states, both spin and parity undetermined level energies, and those of obvious 1^+ states are excluded. Moreover, the level energies at 2.004MeV and 2.158MeV with spin and parity assignments $(1^+, 2^+)$ and $1^+, 2^+$, respectively, are also not included. As shown in Table I, spins of some excited states are not fully confirmed, so that the spin assignments to these states in the theory are tentative, which may be altered according to further experimental results. In addition, some level energies higher than 2.17MeV provided in Table I, such as 3_3^+ at 2.275MeV, 7_1^+ at 2.423MeV, 8_2^+ at 2.689MeV, 10_1^+ at 2.849MeV, and 10_2^+ at 2.917MeV, of which the values are underlined, are for reference only. As noted in [31, 32], the 10^+ state at 2.438MeV seems to be a pair-broken state with major components of proton-holes in $1h_{11/2}$-orbit and neutron-holes in $i_{13/2}$-orbit, which can not be described in this simple model because the interactions between the core described by the IBM and the holes are not considered. According to [23], the other two 10^+ states at 2.849MeV and 2.917MeV may be 10_1^+ and 10_2^+ of the model, respectively, of which the model results are shown in Table I. The quality of the fitting is measured by

$$\chi = \left(\frac{1}{N_l - N_{\text{par}}}\sum_{i=1}^{N_l}(E_{i,\text{th}} - E_{i,\text{exp}})^2\right)^{1/2}, \qquad (48)$$

where N_l is the total number of level energies fitted, N_{par} is the number of parameters used in (40), $E_{i,th}$ and $E_{i,exp}$ are a level energy of the theory and that of the corresponding experimental value, respectively. The number of parameters used in (2) and (40) for ^{194}Pt is $N_{par} = 5$. Except the underlined level energies, there are 33 level energies listed in Table I being fitted, with which we get $\chi = 166.4$keV. The largest absolute deviation in level energies now occurs at 5_2^+ with $|E_{th}(5_2^+) - E_{exp}(5_2^+)| = 422$keV, while absolute deviations of other level energies are all less than 200keV.

In order to check the validity of the theory, the reduced $T(E2)$ matrix elements (32) and (33) are systematically compared with those shown in [23]. We observe that there are a little differences of the experimental B(E2) values provided in [24] from those extracted from the reduced matrix elements of $T(E2)$ shown in [23]. The q_2 parameter is adjusted according to the experimental value of $B(E2, 2_1^+ \to 0_g^+)$ in W. u. given in [24], from which we get $q_2 = 1.3297\sqrt{\text{W.u.}}$ Since the reduced $T(E2)$ matrix elements shown in [23] are in e·b, the standard unit conversion with 1 W. u.$= \frac{1}{4\pi}(3/5)^2 R^4 e^2$, where $R = 1.3A^{1/3}$fm, is used. Hence, $q_2 = 1.3297\sqrt{\text{W.u}}$ is equivalent to $q_2 = 0.12747$ e·b, which is used in this work. While the mixing parameter g and λ are mainly determined from the best fit to $B(E2, 0_4^+ \to 2_1^+)$ and $B(E2, 0_4^+ \to 2_2^+)$ from which we get $\lambda = 0.5$, $\Delta = 0.800$MeV and $g = 0.204$MeV. The reduced $T(E2)$ matrix elements calculated in this work and those shown in [23], together with those in the O(6)-limit without the third order term X_3 are shown in Table II. Since there is always a freedom in choosing an overall phase for any state, the overall phase of the 2_2^+ state in both this work and the original O(6)-limit should be set as -1 according to the experimental result of $\langle 2_1^+ \| T(E2) \| 2_2^+ \rangle$ which is positive as shown in [23]. With this assignment, the inconsistency to the experimental results occurs in $\langle 0_g^+ \| T(E2) \| 2_2^+ \rangle$ in this work, while it is zero in the O(6)-limit due to the fact that it is the selection rule forbidden. Because $\langle 2_2^+ \| T(E2) \| 0_4^+ \rangle$ is related with $\langle 0_g^+ \| T(E2) \| 2_2^+ \rangle$, the sign of $\langle 2_2^+ \| T(E2) \| 0_4^+ \rangle$ obtained in this work is also inconsistent to the corresponding experimental result. Moreover, $\langle 4_1^+ \| T(E2) \| 4_2^+ \rangle$ and $\langle 4_2^+ \| T(E2) \| 6_2^+ \rangle$ in the original O(6)-limit are also inconsistent to the sign determined in [23]. As pointed out in [25], the inconsistency in the sign of the reduced $T(E2)$ matrix elements is common in most collective models, which may be corrected in the IBM-2 as shown in [25]. Except the two opposite signs in $\langle L' \| T(E2) \| L \rangle$ obtained in this work, the overall data pattern of $\langle L' \| T(E2) \| L \rangle$ shown in Table II follows that of the experimental results. Especially, the amplitudes and signs of all diagonal reduced matrix elements of $T(E2)$ obtained in this work agree to the corresponding experimental results.

Table III provides B(E2) values obtained from the reduced matrix elements of $T(E2)$ of this work. Electric quadrupole moments of some low-lying states are also calculated in comparing with those extracted from the diagonal reduced matrix element of $T(E2)$ provided in [23]. The corresponding results obtained from the IBM-CM and ECQF provided in [22] are also shown in Table III for comparison.

As shown in Table III, the overall data pattern of the electric quadrupole moments follows that of the experimental data, especially the sign is now correct, which indicates the third order term being indispensable in describing ^{194}Pt. As shown in (31), mixing of different O(5) seniority number ν occurs in $L \neq 0$ and $L \neq 3$ states with any possible η when the parameter $b \neq 0$, which alters the selection rules of the reduced matrix elements of $\hat{Q}$. Especially, the diagonal reduced matrix elements of $\hat{Q}$ become nonzero when $b \neq 0$. It is observed that the sign of b should be negative according to the sign of the observed electric quadrupole moments of ^{194}Pt. Furthermore, most B(E2) values calculated in this work agree to the experimental values, of which each value is very close to the corresponding result calculated from the IBM-CM. However, $B(E2, 0_2^+ \to 2_2^+)$ is 8 times larger, while $B(E2, 10_2^+ \to 8_1^+)$ is 17 times smaller than the corresponding experimental value. Similar to the IBM-CM result, $B(E2, 0_4^+ \to 2_2^+)$ is still too small. The ECQF with a similar third order term may be adopted to reduce these discrepancies, which is worthy to be considered to describe even-even $^{172-196}$Pt systematically in our future work.

A detailed comparison of the most of the excited level energies up to 3MeV with known absolute B(E2) values obtained in this work to the experimental results [23, 24] is presented in Fig. 3. It can be observed from Fig. 3 that the description of the yrast band including B(E2) values is quite good. Not only the level positions in the quasi-γ and the quasi-β bands, and even the 0_3^+ and 0_5^+ band heads, but also the level positions of the $5_{1,2}^+$, $6_{2,3}^+$, 7_1^+, $8_{1,2}^+$, and $10_{1,2}^+$ are correctly reproduced, which indicates that the moment of inertia is effectively enhanced by the exponential form of the quadrupole-quadrupole interaction. However, the even-odd staggering persists, which may be overcome by using the extended-Q operator to replace the O(6) quadrupole operator.
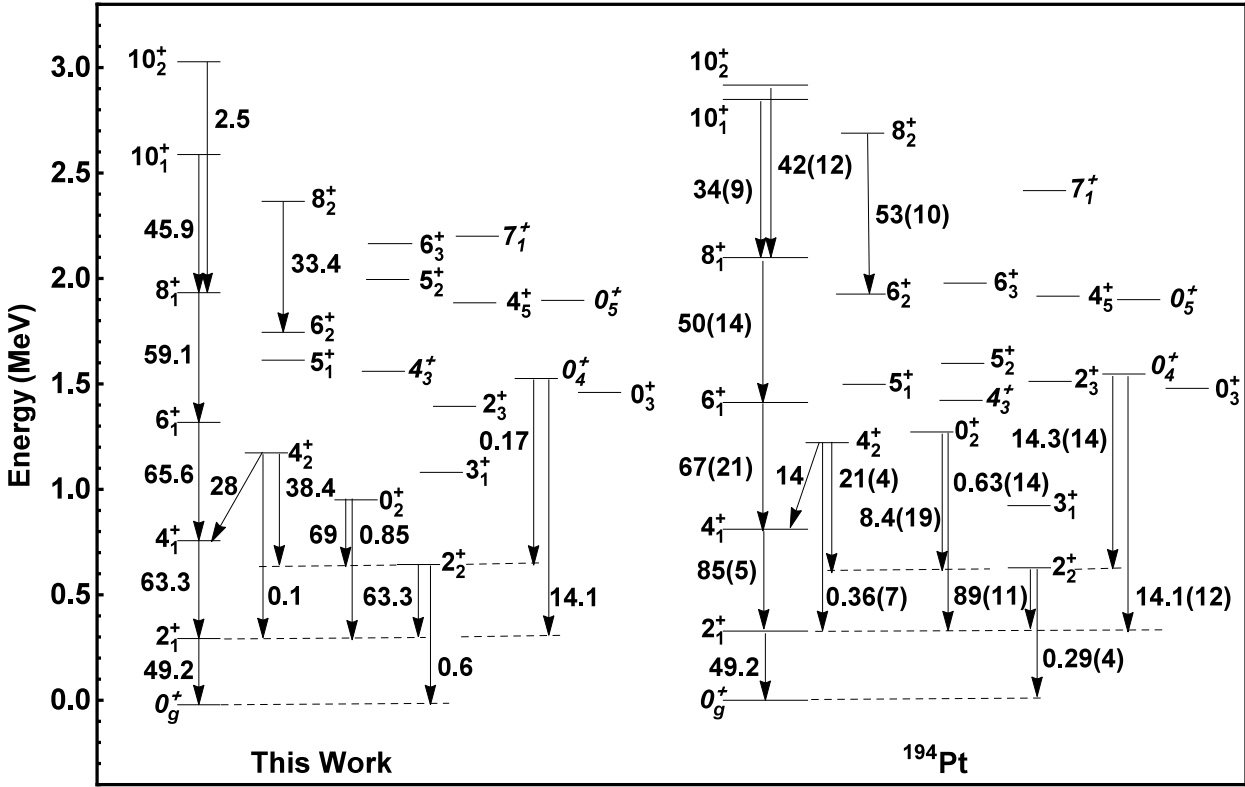
FIG. 3: (Color online) Detailed comparison of the most of the excited level energies up to 3MeV with known absolute B(E2) values in W. u. obtained in this work to the experimental results [23, 24] for ^{194}Pt.

TABLE I: Most of the low-lying positive parity level energies (in MeV) of ^{194}Pt fitted by the Hamiltonians (2) and (40), where $*$ indicates that the the model parameter $\mathbf{\Delta}_{2p2h} = 1.547$ MeV is fixed according to the value of the 0_4^+ level energy, the first column provides the spin ordered according to the value of the level energies for fix L with parity and the corresponding other quantum numbers of the theory, the second column shows the spin and parity determined in experiments (Exp.) [24], the third column gives the level energy calculated in this work, and the fourth column shows the corresponding level energy determined in [24]. Further explanation is shown in the text.

$L^\pi_{\zeta,\sigma,\eta}$	Exp.[24]	This Work	Exp. [24]	$L^\pi_{\zeta,\sigma,\eta}$	Exp. [24]	This Work	Exp. [24]
$2_1^+ = 2_{1,7,1}^+$	2^+	0.314	0.328	$0_3^+ = 0_{1,5,1}^+$	0^+	1.481	1.479
$2_2^+ = 2_{1,7,2}^+$	2^+	0.665	0.622	$2_5^+ = 2_{1,5,1}^+$	2^+	1.754	1.622
$4_1^+ = 4_{1,7,1}^+$	4^+	0.778	0.811	$2_6^+ = 2_{1,5,2}^+$	2^+	1.806	1.671
$0_2^+ = 0_{1,7,2}^+$	0^+	0.982	1.267	$4_4^+ = 4_{1,5,1}^+$	$(2^+,3^+,4^+)$	1.878	1.870
$3_1^+ = 3_{1,7,1}^+$	3^+	1.102	0.923	$0_5^+ = 0_{1,5,2}^+$	(0^+)	1.895	1.893
$4_2^+ = 4_{1,7,2}^+$	4^+	1.183	1.229	$3_2^+ = 3_{1,5,1}^+$	$(0^+,1,2,3^+)$	2.014	2.052
$6_1^+ = 6_{1,7,1}^+$	6^+	1.339	1.412	$4_6^+ = 4_{1,5,2}^+$	(4^+)	2.095	2.126
$2_3^+ = 2_{1,7,3}^+$	2^+	1.415	1.512	$2_9^+ = 2_{1,5,3}^+$	(2^+)	2.099	1.930
$4_3^+ = 4_{1,7,3}^+$	$(3^+,4^+)$	1.575	1.422	$0_7^+ = 0_{1,3,1}^+$	$(0^+,1,2)$	1.991	2.141
$5_1^+ = 5_{1,7,1}^+$	(5^+)	1.634	1.498	$2_8^+ = 2_{1,3,1}^+$	$1^+,2^+$	2.089	1.816
$6_2^+ = 6_{1,7,2}^+$	(6^+)	1.766	1.926	$2_{10}^+ = 2_{1,3,2}^+$	$1^+,2^+$	2.192	2.064
$8_1^+ = 8_{1,7,1}^+$	(8^+)	1.954	2.099	$0_8^+ = 0_{1,1,1}^+$	0^+	2.173	2.164
$2_4^+ = 2_{1,7,4}^+$	$(0^+,1^+,2^+)$	1.642	1.584	$2_{12}^+ = 2_{1,1,1}^+$	$1^+,2^+$	2.266	2.134
$4_5^+ = 4_{1,7,4}^+$	(4^+)	1.888	1.911				
$5_2^+ = 5_{1,7,2}^+$	(5^+)	2.015	1.593	$0_4^+ = 0_{2,7,1}^+$	0^+	1.547^*	1.547
$6_3^+ = 6_{1,7,3}^+$	$(6,7,8^+)$	2.167	1.984	$2_7^+ = 2_{2,7,1}^+$	$1^+,2^+$	1.861	1.803
$7_1^+ = 7_{1,7,1}^+$	$(6^+,7,8^+)$	2.191	2.423	$2_{11}^+ = 2_{2,7,2}^+$	$(1^+,2^+)$	2.212	2.109
$8_2^+ = 8_{1,7,2}^+$	(8^+)	2.387	2.689				
$0_6^+ = 0_{1,7,3}^+$	0^+	1.961	2.085				
$3_3^+ = 3_{1,7,2}^+$	$(2^+,3^+,4^+)$	2.080	2.275				
$10_1^+ = 10_{1,7,1}^+$	(10^+)	2.609	2.849				
$10_2^+ = 10_{1,7,2}^+$	(10^+)	3.049	2.917				

TABLE II: $T(\mathrm{E2})$ matrix elements (in $e\cdot$b), in which the q_2 parameter in this work is adjusted according to the experimental value of $B(\mathrm{E2}, 2_1^+ \to 0_g^+)$ given in [24] with $q_2 = 0.12747$ e·b (see text), while the q_2 parameter for the original O(6)-limit without the third order term X_3 is fixed according to the experimental value of $\langle 0_g^+ \| T(\mathrm{E2}) \| 2_1^+ \rangle$ indicated with *, where † indicates the corresponding sign is opposite to that determined in [23], and the mixing parameter g and λ are mainly determined from the best fit to $B(\mathrm{E2}, 0_4^+ \to 2_1^+)$ and $B(\mathrm{E2}, 0_4^+ \to 2_2^+)$ from which we get $\lambda = 0.5$, $\Delta = 0.800\mathrm{MeV}$ and $g = 0.204\mathrm{MeV}$.

$L \to L'$		$\langle L' \| T(\mathrm{E2}) \| L \rangle$	
	Experiment [23]	This Work	O(6) Limit
$2_1^+ \to 0_g^+$	$(+)\, 1.208^{+49}_{-17}$	1.504	1.208*
$4_1^+ \to 2_1^+$	$(+)\, 1.935^{+21}_{-13}$	2.288	1.874
$6_1^+ \to 4_1^+$	$(+)\, 2.90^{+10}_{-4}$	2.801	2.310
$8_1^+ \to 6_1^+$	$(+)\, 3.08^{+10}_{-16}$	3.039	2.560
$10_1^+ \to 8_1^+$	2.20^{+25}_{-27}	2.976	2.626
$2_2^+ \to 0_g^+$	$+0.0888(12)$	$(-)0.167^\dagger$	0
$2_2^+ \to 2_1^+$	$(+)\, 1.517^{+11}_{-18}$	1.707	1.395
$2_2^+ \to 4_1^+$	$+\, 0.25^{+14}_{-6}$	0.153	0
$4_2^+ \to 2_1^+$	$+\, 0.220(9)$	0.091	0
$4_2^+ \to 4_1^+$	$+\, 1.51^{+6}_{-5}$	1.521	$(-)\, 1.327^\dagger$
$4_2^+ \to 6_1^+$	$+\, 0.16^{+6}_{-16}$	0.148	0
$4_2^+ \to 2_2^+$	$(+)\, 1.784^{+45}_{-29}$	1.781	1.391
$6_2^+ \to 4_1^+$	$\pm\, 0.224^{+17}_{-19}$	-0.553	0
$6_2^+ \to 6_1^+$	$+\, 1.14^{+11}_{-24}$	1.430	1.271
$6_2^+ \to 4_2^+$	$(+)\, 2.09^{+11}_{-7}$	2.177	$(-)1.860^\dagger$
$8_2^+ \to 6_2^+$	$(+)\, 2.44^{+28}_{-15}$	2.284	2.071
$10_2^+ \to 8_1^+$	2.43^{+32}_{-41}	0.698	0
$0_2^+ \to 2_1^+$	$\pm\, 0.070^{+9}_{-15}$	0.088	0
$0_2^+ \to 2_2^+$	$(+)\, 0.231^{+30}_{-21}$	0.798	0.6446
$2_1^+ \to 2_1^+$	$+\, 0.54^{+8}_{-6}$	0.382	0
$4_1^+ \to 4_1^+$	$+\, 1.00^{+12}_{-14}$	0.775	0
$6_1^+ \to 6_1^+$	$+\, 0.28^{+12}_{-27}$	1.549	0
$8_1^+ \to 8_1^+$	$-\, 0.10,\ 0.43$	1.452	0
$2_2^+ \to 2_2^+$	$-\, 0.40^{+12}_{-5}$	-0.382	0
$4_2^+ \to 4_2^+$	$-\, 0.07(14)$	-0.046	0
$6_2^+ \to 6_2^+$	$+\, 0.41^{+26}_{-22}$	0.180	0
$0_4^+ \to 2_1^+$	$+\, 0.309^{+9}_{-10}$	0.360	0.2907
$0_4^+ \to 2_2^+$	$(+)\, 0.304^{+11}_{-9}$	$(-)0.040^\dagger$	0

TABLE III: Some absolute (the first part) and relative (the second part for the transitions from the 3_1^+ state) B(E2) values (in W. u) and electric quadrupole moments (in $e \cdot b$) (the third part) of ^{194}Pt fitted by this model and compared with experimental data and the fitting results of the IBM-CM and ECQF shown in [22], where * indicates the q_2 parameter is adjusted according to the corresponding experimental value with $q_2 = 1.3297\sqrt{\text{W.u}}$ or equivalently with $q_2 = 0.12747$ e·b used in Table II, − indicates that the corresponding value was not calculated.

$L \to L'$	Experiments [23, 24]	This Work	IBM-CM [22]	ECQF [22]
$2_1^+ \to 0_g^+$	49.2(8)	49.2*	49.6	49
$4_1^+ \to 2_1^+$	85(5)	63.3	66	67
$6_1^+ \to 4_1^+$	67(21)	65.6	67	72
$8_1^+ \to 6_1^+$	50(14)	59.1	−	−
$10_1^+ \to 8_1^+$	34(9)	45.9	−	−
$2_2^+ \to 0_g^+$	0.29(4)	0.6	0	0.21
$2_2^+ \to 2_1^+$	89(11)	63.3	66	63
$4_2^+ \to 4_1^+$	14	28	32	33
$4_2^+ \to 2_1^+$	0.36(7)	0.1	0	0
$4_2^+ \to 2_2^+$	21(4)	38.4	35	37
$8_2^+ \to 6_2^+$	53(10)	33.4	−	−
$10_2^+ \to 8_1^+$	42(12)	2.5	−	−
$0_2^+ \to 2_1^+$	0.63(14)	0.85	0.91	4.5
$0_2^+ \to 2_2^+$	8.4(19)	69	9.2	39
$0_4^+ \to 2_1^+$	14.1(12)	14.1	14	0.02
$0_4^+ \to 2_2^+$	14.3(14)	0.17	0	0
$3_1^+ \to 4_1^+$	< 75	35.1	40	39
$3_1^+ \to 2_2^+$	100	100	100	100
$3_1^+ \to 2_1^+$	< 0.64	1.2	0.0	0.6
$Q(2_1^+)$	$+\,0.409\left(^{+62}_{-43}\right)$	0.2895	0	-0.288
$Q(4_1^+)$	$+\,0.752\left(^{+92}_{-105}\right)$	0.5841	0	-0.308
$Q(6_1^+)$	$+\,0.195\left(^{+85}_{-188}\right)$	1.0798	0	-0.284
$Q(8_1^+)$	$-\,0.06,\ 0.28$	0.9357	0	-0.26
$Q(2_2^+)$	$-\,0.303\left(^{+93}_{-37}\right)$	-0.2897	0	0.259
$Q(4_2^+)$	$-\,0.06\ (11)$	-0.0350	0	0.09
$Q(6_2^+)$	$+\,0.286\left(^{+181}_{-153}\right)$	0.1258	−	−

4. Conclusions

In this paper, in order to describe obvious intruder states and nonzero quadrupole moments of γ-soft nuclei such as ^{194}Pt, a rotor extension plus intruder configuration mixing with $2n$-particle and $2n$-hole configurations from $n = 0$ up to $n \to \infty$ in the O(6) (γ-unstable) limit of the interacting boson model is proposed. The configuration mixing scheme keeps lower part of the γ-unstable spectrum unchanged and generates the intruder states due to the mixing. The main feature of this exactly solvable configuration mixing scheme lies in the fact that the O(6) pairing operator is used in the configuration mixing term, which greatly simplifies the calculation in the O(6)-limit of the IBM and keeps the nature of the $2n$-particle and $2n$-hole excitations unchanged. As a result, the eigenstates of the model Hamiltonian are the SU(1,1) coherent states built on the O(6)-limit states of the IBM. Hence, matrix elements of physical quantities can be derived analytically. Furthermore, we observe the exponential form of the O(6) quadrupole-quadrupole interaction is important to enhance the moment of inertia, with which level energies with high d-boson seniority quantum number can be correctly reproduced. In order to reproduce nonzero quadrupole moments of ^{194}Pt with the correct sign, the third order term needed for a rotor realization in the IBM seems indispensable. A detailed analysis of low energy spectrum of ^{194}Pt up to 2.17MeV shows that the γ-soft rotor model with configuration mixing proposed in this paper are better in reproducing correct positions of the level energies, B(E2) values, and electric quadrupole moments,

especially the sign of the quadrupole moments becomes correct. Though there are a few discrepancies, such as incorrect amplitude of a few B(E2) values, level energy staggering in the quasi-γ band, and opposite sign in a few reduced T(E2) matrix elements, the model description of ^{194}Pt is greatly improved. It can be expected that these discrepancies may be overcome by using the extended consistent-Q formalism with the configuration mixing, which is worthy to be considered to describe even-even $^{172-196}$Pt systematically in our future work.

Acknowledgements

[1] F. Iachello and A. Arima, The Interacting Boson Model (Cambridge University Press, Cambridge, 1987).
[2] K. Heyde, P. Van Isacker, M. Waroquier, J. L. Wood, and R. A. Meyer, Phys. Rep. **102** (1983) 291.
[3] J. L. Wood, K. Heyde, W. Nazarewicz, M. Huyse, and P. Van Duppen, Phys. Rep. **215** (1992) 101.
[4] K. Heyde and J. L. Wood, Rev. Mod. Phys. **83** (2011) 1467; 1655.
[5] P. D. Duval and B. R. Barrett, Phys. Lett. B **100** (1981) 223.
[6] P. D. Duval and B. R. Barrett, Nucl. Phys. A **376** (1982) 213.
[7] K. Heyde, P. Van Isacker, J. Jolie, J. Moreau and M. Waroquier, Phys. Lett. B **132** (1983) 15.
[8] K. Heyde, J. Jolie, P. Van Isacker, J. Moreau and M. Waroquier, Phys. Rev. C **29** (1984) 1428.
[9] P. Van Isacker, S. Pittel, A. Frank, and P. D. Duval, Nucl. Phys. A **451** (1986) 202.
[10] K. Heyde, J. Jolie, J. Moreau, J. Ryckebush, M. Waroquier, P. Van Duppen, M. Huyse, and J. L. Wood, Nucl. Phys. A **466** (1987) 189.
[11] C. De Coster, K. Heyde, B. Decroix, P. Van Isacker, J. Jolie, H. Lehmann, J. L. Wood, Nucl. Phys. A **600** (1996) 251.
[12] H. Lehmann, J. Jolie, C. De Coster, B. Decroix, K. Heyde, J. L. Wood, Nucl. Phys. A **621** (1997) 767.
[13] K. Nomura, T. Otsuka, and P Van Isacker, J. Phys. G: Nucl. Part. **43** (2016) 024008.
[14] T. Thomas, V. Werner, J. Jolie, K. Nomura, T. Ahn, N. Cooper, H. Duckwitz, A. Fitzler, C. Fransen, A. Gade, M. Hinton, G. Ilie, K. Jessen, A. Linnemann, P. Petkov, N. Pietralla, D. Radeck, Nucl. Phys. A **947** (2016) 203.
[15] Y. F. Smirnov, N. A. Smirnova, and P. Van Isacker, Phys. Rev. C **61** (2000) 041302(R).
[16] Y. Zhang, F. Pan, L.-R. Dai, and J. P. Draayer, Phys. Rev. C **90** (2014) 044310.
[17] F. Pan and J. P. Draayer, Nucl. Phys. A **636** (1998) 156.
[18] G. Thiamova and D. J. Rowe, Eur. Phys. J. A **41** (2009) 189.
[19] D. J. Rowe and P. S. Turner, J. Math. Phys. **45** (2004) 2761.
[20] F. Pan, L. Bao, Y.-Z. Zhang and J. P. Draayer, Eur. Phys. J. Plus **129** (2014) 169.
[21] E. A. McCutchan, R. F. Casten, and N. V. Zamfir, Phys. Rev. C **71** (2005) 061301(R).
[22] J. E. Garcia-Ramos and K. Heyde, Nucl. Phys. A **825** (2009) 39.
[23] C. Y. Wu, D. Cline, T. Czosnyka, A. Backlin, C. Baktash, R. M. Diamond, G. D. Dracoulis, L. Hasselgren, H. Kluge, B. Kotlinski, J. R. Leigh, J. O. Newton, W. R. Phillips, S. H. Sie, J. Srebrny, F. S. Stephens, Nucl. Phys. A **607** (1996) 178.
[24] B. Singh, Nucl. Data Sheets **107** (2006) 1531.
[25] R. Bijker, A. E. L. Dieperink, and O. Scholten, Nucl. Phys. A **344** (1980) 207.
[26] G. K. Tobin, M. C. Ferriss, K. D. Launey, T. Dytrych, J. P. Draayer, A. C. Dreyfuss, and C. Bahri, Phys. Rev. C **89** (2014) 034312.
[27] R. Gilmore, J. Math. Phys. **20**, 891 (1979).
[28] J. N. Ginocchio and M. W. Kirson, Phys. Rev. Lett. **44**, 1744 (1980).
[29] A. E. L. Dieperink, O. Scholten, and F. Iachello, Phys. Rev. Lett. **44**, 1747 (1980).
[30] P. Van Isacker and J. Q. Chen, Phys. Rev. C **24** (1981) 684.
[31] M. Piiparinen, J. C. Cunnane, P. J. Daly, C. L. Dors, F. M. Bernthal, and T. L. Khoo, Phys. Rev. Lett. **34** (1975) 1110.
[32] S. A. Hjorth, A. Johnson, T. Lindblad, L. Funke, P. Kemnitz, and G. Winter, Nucl. Phys. A **262** (1976) 328.